Bulletin of the Seismological Society of America, Vol. 96, No. 1, pp. 348–354, February 2006, doi: 10.1785/0120040086

Q_{L_g} Distribution in the Basin and Range Province of the Western United States

by Ghassan I. Aleqabi and Michael E. Wysession

Abstract Q values for the direct L_g phase (Q_{L_g}) were estimated for event-station paths that lie entirely within the western United States, particularly in the southern Great Basin and surrounding areas. The Q_o (Q_{L_g} at 1 Hz) values were estimated by fitting synthetic spectra to observed L_g spectra using a genetic algorithm technique. We have created a tomographic image of the variations of Q_o for a part of the southwestern United States. The image shows that Q_o varies between about 234 and 312 at 1 Hz, with an average of 267. The lowest Q_o occurs in the northwest part of the Basin and Range Province, where extensional deformation has occurred since the Mesozoic. Q_o values start to increase toward the Colorado Plateau to the east and continue to gradually increase northward and decrease southward. We also find relatively high frequency dependence to the Q_{L_g} values, with a 1D mean of $\eta = 0.57$.

Introduction

We present the results of a study of crustal attenuation in the southwestern United States using the L_g waves from regional earthquakes and nuclear tests (Fig. 1). The region of study encompasses part of the Basin and Range Province, as well as the southeastern part of the Sierra-Nevadas. The diversity of tectonic regimes in the western United States causes variations in the propagation and attenuation of seismic waves. Mitchell (1995) showed that the time elapsed since the most recent significant tectonic activity in a region is important in determining the attenuation properties there. Areas that have undergone more recent tectonism tend to be more attenuating. In addition, factors that increase attenuation of regional seismic phases include the presence of a thick cover of low Q sediments and velocity gradients (rather than a sharp interface) at the crust–mantle boundary (Mitchell and Cong, 1998). Attenuation is very sensitive to increases in temperature, and so attenuation tomography is well suited for identifying thermal anomalies.

Studies of L_g propagation from earthquake and explosion sources in the Basin and Range Province have reported regional variations in Q_{L_g} values. In a prior study we calculated the moment and corner frequency for 40 seismic sources (Al-Eqabi *et al.*, 2001). In this article we also calculate Q_o (Q_{L_g} at 1 Hz) and η (the frequency dependence) and relate the crustal anelastic properties to the tectonic evolution and geology of the Basin and Range Province. We further apply the back-projection inversion technique to obtain a tomographic map of Q_o variations in the Basin and Range Province and its surroundings.

Data

Our dataset consists of 111 vertical-component seismograms from 40 regional seismic events between 1988 and 1994 (table 3 in Al-Eqabi *et al.*, 2001). Fifteen of these events were Nevada Test Site (NTS) nuclear explosions, and 25 were western U.S. earthquakes. To process the data, L_g spectra were isolated in a manner similar to that used by Chael (1987) and Atkinson and Mereu (1992). The individual source-station Q_o values were obtained by applying the L_g spectral fit by a genetic algorithm (LGSFGA) technique (Al-Eqabi *et al.*, 2001). The LGSFGA method was developed to analyze the L_g amplitude spectrum in terms of four independent variables: the seismic moment, corner frequency of the seismic source, average path attenuation at 1 Hz (Q_o), and attenuation frequency dependence (η). A genetic algorithm was used to efficiently search the parameter space and find optimum combinations of the four parameters to produce a calculated spectrum that best fit the observed L_g spectrum. The resulting Q_o and η values along with event information are given in Table 1. While the genetic algorithm is efficient in finding solutions that provide the least misfit to the observed spectra, it must be remembered that noise in the signals and effects from structural heterogeneities can result in a trade-off between the attenuation values and the corner frequency. There are other factors, such as geometric spreading, that can also provide a source of contamination for the individual path attenuation values. However, a consistent technique has been applied across all of the data, and so contaminating effects have been addressed as evenly as possible, but they are always a concern.

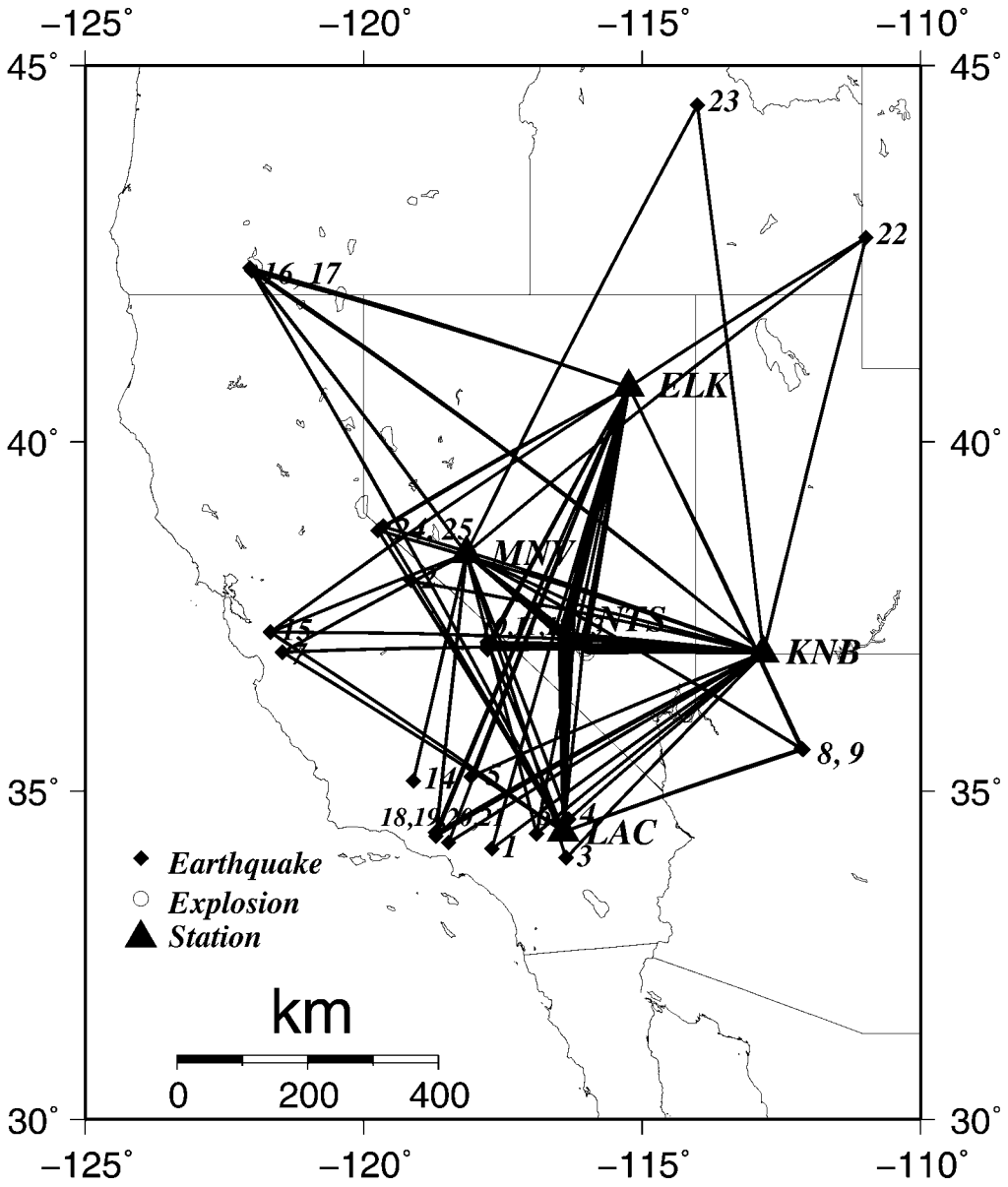

Figure 1. Ray paths used in the tomographic inversion. Earthquakes are represented by diamonds, NTS explosions by circles, and Lawrence Livermore National Laboratory stations by triangles. Numbers indicate each event identification number (table 3 in Al-Eqabi *et al.*, 2001).

Figure 1 shows the ray-path distribution within the area of study. Data coverage across the Basin and Range Province and its surroundings is not uniform because the earthquakes are mostly located in the southern Basin and Range and California coastal region, and the explosions are clustered inside the NTS. The coverage is best in the southern Basin and Range, while the northeastern part of the Basin and Range is poorly sampled.

Q_{Lg} Tomography

Utilizing the assembled Q_o values for each event-station pair (Table 1), we used the back-projection tomographic method (Xie and Mitchell, 1990a; Cong and Mitchell, 1998; L. Cong, personal comm., 2000) to create a tomographic image of the distribution of Q_o over the region of study. This technique requires that the area of study be divided into a grid of rectangular cells, so we divided the area spanning latitudes 34–41° N and longitudes 113–120° W into 49 1° × 1° cells (N_c). Then we calculated Q_n, the Q_o value calculated for the nth time series $n = 1,2,3, \ldots, N_d$, for each cell m according to

$$\frac{1}{Q_n} = \frac{1}{L_n} \sum_{m=1}^{N_c} \frac{l_{mn}}{Q_m} + \varepsilon_n, \quad n = 1, 2, 3, \ldots, N_d, \quad (1)$$

Table 1
Earthquakes and Explosions in Western United States with Results of LGSFGA Technique

Date (mm/dd/yy)	Origin Time (h:m:s)	Latitude	Longitude	Recording Station	Distance (km)	Q_o	η
08/11/93	22:33:04.00	37.313	−121.675	ELK	674.5	277	0.59
12/04/92	02:08:57.50	34.369	−116.897	ELK	722.6	341	0.53
02/03/94	09:05:04.20	42.762	−110.976	ELK	418.7	140	0.67
05/18/93	23:48:53.90	37.064	−117.777	ELK	464.1	245	0.70
05/19/93	14:13:22.58	37.137	−117.768	ELK	456.6	229	0.67
05/18/93	01:03:06.43	37.152	−117.762	ELK	454.9	237	0.56
07/11/92	18:14:16.15	35.210	−118.066	ELK	662.6	332	0.53
09/21/93	03:28:55.42	42.314	−122.012	ELK	591.4	188	0.70
09/21/93	05:45:33.75	42.358	−122.045	ELK	595.3	188	0.73
01/17/94	23:33:30.69	34.326	−118.698	ELK	775.7	350	0.62
01/18/94	00:43:08.79	34.377	−118.698	ELK	769.4	333	0.59
01/19/94	21:09:28.59	34.379	−118.711	ELK	770.1	350	0.62
03/20/94	21:20:12.20	34.231	−118.475	ELK	777.4	269	0.65
02/28/90	23:43:36.60	34.140	−117.700	ELK	764.6	350	0.53
04/29/93	08:21:00.81	35.611	−112.112	ELK	633.8	317	0.53
04/25/93	09:29:50.30	35.624	−112.147	ELK	632.6	350	0.44
09/12/94	12:23:43.20	38.819	−119.652	ELK	434.3	301	0.47
09/12/94	23:57:09.84	38.759	−119.744	ELK	444.6	317	0.56
07/07/88	15:05:30.07	37.252	−116.377	ELK	400.1	293	0.47
11/14/90	19:17:00.07	37.227	−116.371	ELK	397.0	261	0.79
08/17/88	17:00:00.09	37.297	−116.307	ELK	393.8	261	0.56
06/27/89	15:30:00.00	37.275	−116.354	ELK	397.0	309	0.59
05/13/90	15:34:59.99	37.262	−116.420	ELK	400.0	333	0.67
06/22/89	21:15:00.00	37.283	−116.412	ELK	397.5	180	0.56
10/31/89	15:30:00.00	37.263	−116.490	ELK	401.4	341	0.73
03/09/89	14:05:00.00	37.143	−116.067	ELK	406.3	196	0.70
03/10/90	16:00:00.00	37.112	−116.055	ELK	409.5	221	0.70
07/25/90	15:00:00.00	37.720	−116.210	ELK	401.7	317	0.99
02/10/89	20:30:00.00	37.077	−116.000	ELK	412.5	269	0.53
08/11/93	22:33:04.00	37.313	−121.675	KNB	786.2	350	0.53
12/04/92	02:08:57.50	34.369	−116.897	KNB	471.4	333	0.39
02/03/94	09:05:04.20	42.762	−110.976	KNB	656.4	212	0.67
05/17/93	23:20:49.22	37.171	−117.775	KNB	440.6	164	0.62
05/18/93	23:48:53.90	37.064	−117.777	KNB	440.8	293	0.56
05/19/93	14:13:22.58	37.137	−117.768	KNB	439.9	309	0.56
05/18/93	01:03:06.43	37.152	−117.762	KNB	439.4	333	0.33
07/11/92	18:14:16.15	35.210	−118.066	KNB	512.8	332	0.42
01/16/93	06:29:34.90	37.025	−121.458	KNB	768.2	341	0.53
06/07/94	13:30:03.47	44.493	−114.003	KNB	835.7	277	0.62
09/21/93	03:28:55.42	42.314	−122.012	KNB	982.8	293	0.70
09/21/93	05:45:33.75	42.358	−122.045	KNB	987.8	325	0.70
06/30/92	14:38:11.59	34.004	−116.361	KNB	463.4	317	0.70
07/05/92	21:18:27.09	34.583	−116.319	KNB	415.6	212	0.76
10/24/90	06:15:12.70	38.047	−119.157	KNB	571.3	317	0.85
01/17/94	23:33:30.69	34.326	−118.698	KNB	610.5	293	0.62
01/18/94	00:43:08.79	34.377	−118.698	KNB	606.3	253	0.53
01/19/94	21:09:28.59	34.379	−118.711	KNB	607.9	204	0.65
03/20/94	21:20:12.20	34.231	−118.475	KNB	597.9	237	0.59
02/28/90	23:43:36.60	34.140	−117.700	KNB	545.2	188	0.62
09/12/94	12:23:43.20	38.819	−119.652	KNB	632.8	350	0.53
09/12/94	23:57:09.84	38.759	−119.744	KNB	638.7	293	0.59
07/07/88	15:05:30.07	37.252	−116.377	KNB	316.9	204	0.53
09/23/92	15:04:00.00	37.021	−115.988	KNB	281.7	317	0.16
11/14/90	19:17:00.07	37.227	−116.371	KNB	314.7	333	0.44
08/17/88	17:00:00.09	37.297	−116.307	KNB	311.0	245	0.44
05/13/88	15:35:00.11	37.124	−116.072	KNB	289.2	293	0.21
06/27/89	15:30:00.00	37.275	−116.354	KNB	314.7	350	0.56
04/04/91	15:34:59.99	37.296	−116.313	KNB	311.3	333	0.50
05/13/90	15:34:59.99	37.262	−116.420	KNB	320.8	341	0.53
06/22/89	21:15:00.00	37.283	−116.412	KNB	320.0	180	0.65

(*continued*)

Table 1
Continued

Date (mm/dd/yy)	Origin Time (h:m:s)	Latitude	Longitude	Recording Station	Distance (km)	Q_o	η
10/31/89	15:30:00.00	37.263	−116.490	KNB	327.0	333	0.56
03/09/89	14:05:00.00	37.143	−116.067	KNB	288.8	333	0.44
03/26/92	16:30:00.99	37.272	−116.360	KNB	315.6	350	0.56
03/10/90	16:00:00.00	37.112	−116.055	KNB	288.1	317	0.56
07/25/90	15:00:00.00	37.720	−116.210	KNB	301.8	301	0.82
02/10/89	20:30:00.00	37.077	−116.000	KNB	282.8	350	0.47
08/11/93	22:33:04.00	37.313	−121.675	MNV	333.3	269	0.33
05/28/93	04:47:40.60	35.149	−119.104	MNV	374.0	261	0.39
12/04/92	02:08:57.50	34.369	−116.897	MNV	464.8	253	0.56
02/03/94	09:05:04.20	42.762	−110.976	MNV	773.8	253	0.67
01/16/93	06:29:34.90	37.025	−121.458	MNV	330.4	309	0.27
06/07/94	13:30:03.47	44.493	−114.003	MNV	756.4	301	0.53
09/21/93	03:28:55.42	42.314	−122.012	MNV	541.3	156	0.70
09/21/93	05:45:33.75	42.358	−122.045	MNV	546.8	156	0.73
06/30/92	14:38:11.59	34.004	−116.361	MNV	517.1	277	0.76
07/05/92	21:18:27.09	34.583	−116.319	MNV	457.6	148	0.85
01/17/94	23:33:30.69	34.326	−118.698	MNV	458.8	180	0.67
01/18/94	00:43:08.79	34.377	−118.698	MNV	452.4	204	0.56
04/29/93	08:21:00.81	35.611	−112.112	MNV	622.0	277	0.53
04/25/93	09:29:50.30	35.624	−112.147	MNV	620.5	277	0.53
07/07/88	15:05:30.07	37.252	−116.377	MNV	204.0	261	0.27
09/23/92	15:04:00.00	37.021	−115.988	MNV	247.0	277	0.10
08/17/88	17:00:00.09	37.297	−116.307	MNV	205.7	293	0.21
05/13/88	15:35:00.11	37.124	−116.072	MNV	234.0	237	0.27
06/27/89	15:30:00.00	37.275	−116.354	MNV	204.2	164	0.59
04/04/91	15:34:59.99	37.296	−116.313	MNV	205.5	229	0.62
05/13/90	15:34:59.99	37.262	−116.420	MNV	200.5	221	0.53
10/31/89	15:30:00.00	37.263	−116.490	MNV	195.7	196	0.53
03/09/89	14:05:00.00	37.143	−116.067	MNV	233.0	196	0.44
03/26/92	16:30:00.99	37.272	−116.360	MNV	203.8	196	0.44
03/10/90	16:00:00.00	37.112	−116.055	MNV	235.6	269	0.42
07/25/90	15:00:00.00	37.720	−116.210	MNV	218.6	301	0.96
02/10/89	20:30:00.00	37.077	−116.000	MNV	242.2	245	0.44
08/11/93	22:33:04.00	37.313	−121.675	LAC	575.0	269	0.53
05/17/93	23:20:49.22	37.171	−117.775	LAC	332.3	350	0.36
01/16/93	06:29:34.90	37.025	−121.458	LAC	542.1	261	0.53
09/21/93	03:28:55.42	42.314	−122.012	LAC	1006.0	237	0.79
09/21/93	05:45:33.75	42.358	−122.045	LAC	1011.7	261	0.76
10/24/90	06:15:12.70	38.047	−119.157	LAC	474.9	350	0.88
04/29/93	08:21:00.81	35.611	−112.112	LAC	414.9	285	0.42
04/25/93	09:29:50.30	35.624	−112.147	LAC	411.8	237	0.53
09/12/94	12:23:43.20	38.819	−119.652	LAC	570.6	261	0.53
09/12/94	23:57:09.84	38.759	−119.744	LAC	569.2	196	0.65
11/14/90	19:17:00.07	37.227	−116.371	LAC	320.2	350	0.47
08/17/88	17:00:00.09	37.297	−116.307	LAC	322.7	188	0.56
04/04/91	15:34:59.99	37.296	−116.313	LAC	322.6	204	0.85
05/13/90	15:34:59.99	37.262	−116.420	LAC	318.7	156	0.79
10/31/89	15:30:00.00	37.263	−116.490	LAC	318.9	229	0.53
03/26/92	16:30:00.99	37.272	−116.360	LAC	319.8	221	0.62
03/10/90	16:00:00.00	37.112	−116.055	LAC	303.8	204	0.70
07/25/90	15:00:00.00	37.720	−116.210	LAC	313.1	269	0.76
05/13/88	15:35:00.11	37.124	−116.072	LAC	304.9	196	0.44

where l_{mn} is the path length in each cell, Q_m is the Q_o for each cell, ε_n is a term signifying the error in measurement and modeling of Q_{L_g}, N_d is the total number of seismic records, and L_n is the event-station path length as defined by

$$L_n = \sum_{j=1}^{N_c} l_{jn}. \quad (2)$$

At the beginning of the inversion ($i = 0$), Q_m^i was set to 270, which is the median value between the lowest and the

highest Q_o for all the paths. For the nth record, a residual term Δ_n^i is calculated using

$$\Delta_n^i = \frac{L_n}{Q_n} - \sum_{m=1}^{N_c} \frac{1}{Q_m^i} l_{mn}. \quad (3)$$

A new estimate of Q_m for each grid, Q_m^{i+1}, is found by back-projecting Δ_n^i into the inverse of Q_m. The residual term is redistributed back to the cells using

$$\frac{1}{Q_m^{i+1}} = \frac{1}{Q_m^i} + \frac{1}{N_i} \sum_{n=1}^{N_d} \Delta_n^i \frac{l_{mn}}{\sum_{j=1}^{N_c} l_{jn}^2}. \quad (4)$$

After experimentation, we found that 20 iterations ($i = 20$) were sufficient to provide stable Q_m values.

Results

The inversion yielded a tomographic map of Q_o for the Basin and Range Province (Fig. 2). The Q_o map exhibits moderate variations in Q_o within the area of study, with an average of 267 and a range of block values between 234 and 312. The result suggests a southwest to northeast trend in the attenuation. The highest Q_o values (286–312) occur in the northeastern and eastern areas of the NTS, and they decrease smoothly to the southwest. The poor path coverage in the northeastern part of the region might have biased the Q_{L_g} values we obtained for this area. All values higher than the average lie to the east and north of the NTS, while the lowest values are concentrated to the south and southwest of the NTS. The higher Q_{L_g} values seem to be associated with the east-central Basin and Range and western part of the Colorado Plateau. This pattern of Q_{L_g} is consistent with the distribution of L_g coda Q variations obtained by Baqer and Mitchell (1998).

Mitchell (1995) and Mitchell and Cong (1998) found that crustal Q_o values of any region are directly proportional to the length of time elapsed since the most recent crustal event that produced substantial metamorphism and associated fluid release. They considered regions (including the Basin and Range Province) with Q for L_g coda ($Q_{L_g}^c$) values between 250 and 333 as still tectonically active. Thus the relatively low Q_o values found in this study would characterize a region that is still tectonically or orogenically active.

While the observed range of Q_o values in the Basin and Range Province indicates a region of active deformation, these variations could also be due to other factors such as intrinsic crustal attenuation, increased relative stability and age of volcanism across the Basin and Range Province, and variations in the accumulated sediment thickness, permeability, and age. Two other competing mechanisms may also have caused enhanced attenuation of seismic energy in the Basin and Range Province. One possibility is the presense of interstitial fluids, due to either reactions at depth caused by high geothermal gradients or the circulation of fluids from shallow sources driven by the geothermal gradient (Wyllie, 1988). The second explanation for enhanced attenuation in the Basin and Range Province associates the region's large-scale extension, higher-than-normal heat-flow values, elevated upper-mantle temperatures, and abundant intrusive and extrusive igneous activity during the Cenozoic with the presence of fluid inclusions and partial melt.

Substantial frequency dependence of attenuation is also observed in the area as indicated by the η values (Table 1). The η values predominantly vary between 0.4 and 0.8 across the region, with an average of 0.57 and most falling in the range of 0.40 to 0.62. Studies have associated low η values (<0.3) with shields and higher values with tectonically active regions (Mitchell, 1995; Baumont *et al.*, 1999). Our higher η values, suggesting a significant frequency-dependent attenuation of Q_{L_g}, are therefore expected since the region is tectonically active.

Discussion and Conclusions

A preliminary study using L_g waves from 40 regional seismic events has investigated the crustal attenuation structure in the southwestern United States. Individual path attenuation values were determined using a new genetic algorithm that simultaneously fits the source spectra for path attenuation (Q_{L_g} and the frequency dependence η) as well as corner frequency and magnitude (Al-Eqabi *et al.*, 2001). These Q_{L_g} values have been inverted for the crustal attenuation structure of a portion of the Basin and Range region.

While uncertainties in the attenuation measurements prevent a direct tectonic interpretation for each anomaly on the map, the major trends of the inversion are likely robust, and agree well with previous studies. The Q_{L_g} values for individual paths vary between 140 and 350 for frequencies from 0.3 to 10 Hz, and when inverted, the mean value for our Q_{L_g} map (267) agrees very well with previous estimates, which are listed in Table 2. For instance, the study of Benz *et al.* (1997) obtained a Q-value of 235 ± 11 for the Basin and Range Province. Several studies have determined Q for L_g waves (Q_{L_g}) or coda ($Q_{L_g}^c$) in the Basin and Range Province. Reported Q_{L_g} and $Q_{L_g}^c$ values vary between 138 and 774, but most studies put the Q-values between 200 and 280. In addition, the significant southwest–northeast trend in increasing Q, ranging between 234 and 312, agrees with the previous work of Baqer and Mitchell (1998).

We tested the success of the tomographic attenuation model in fitting the amplitude data by examining the reduction of the variance of the individual data. We first computed the variance of the data relative to a uniform model with $Q = 267$ everywhere (summing the squares of the differences between the individual path Q^{-1} values and the averaged $Q^{-1} = 1/267$). We then determined Q^{-1} for each path through the tomographic model, by summing Q^{-1} for each block segment along a path, and computed the variance of the data path Q^{-1} values and the tomographic-model Q^{-1}

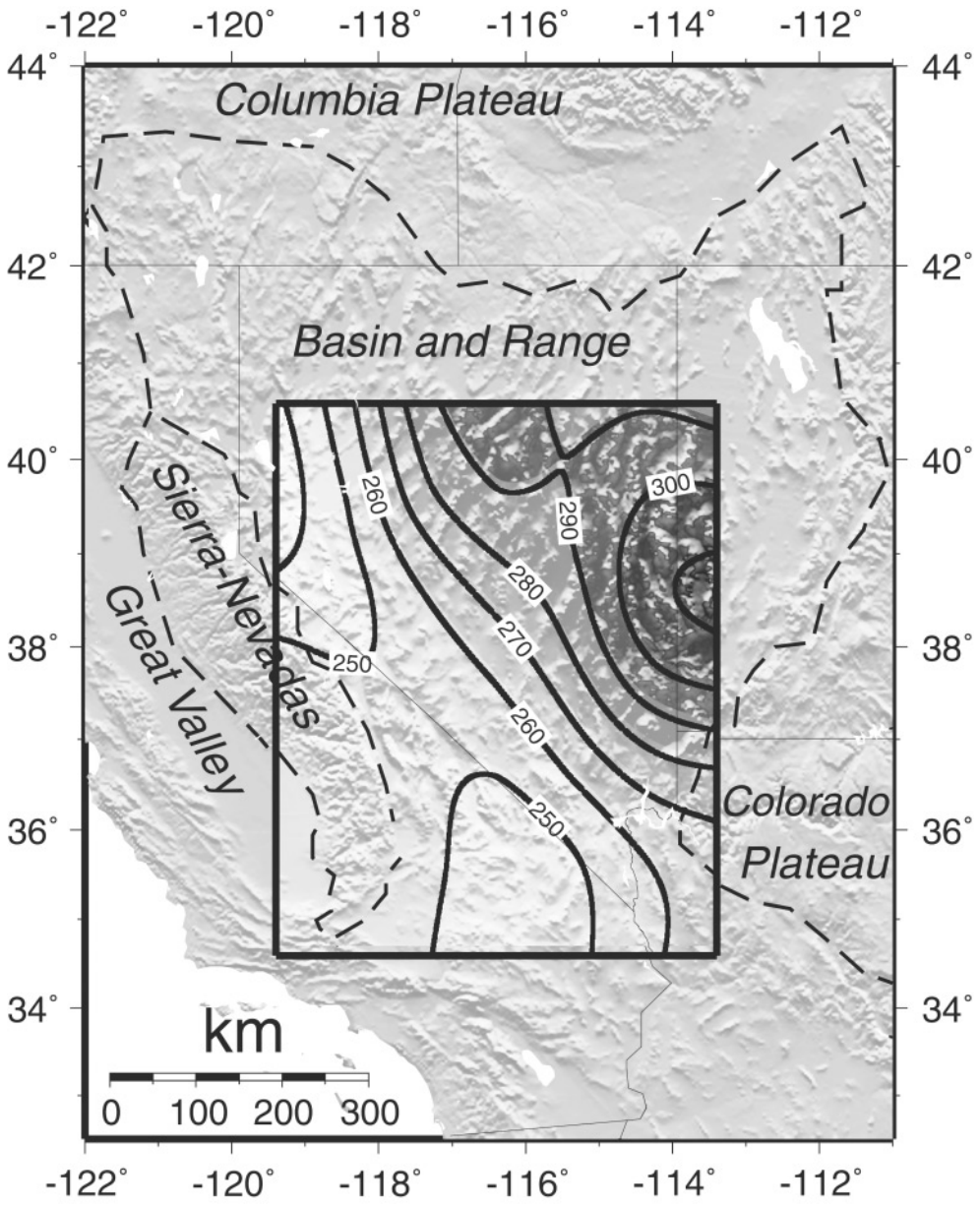

Figure 2. Q_{L_g} from tomographic inversion of L_g amplitudes. Darker shades represent areas of relatively high Q_{L_g}, and lighter shades show areas of low Q_{L_g}, which probably indicates high crustal temperatures. The shades and Q_{L_g} contour lines are superimposed on a topography gradient map with dashed boundaries distinguish various tectonic provinces.

Table 2
Summary of Attenuation Parameters in the Basin and Range Province

Reference	Q_{L_g}	$Q^c_{L_g}$	Q_o	η
Baqer and Mitchell (1998)		250–300		0.40–0.60
Singh and Herrmann (1983)		200–300		0.40–0.60
Chavez and Priestley (1986)	214 ± 15			0.54
Xie and Mitchell (1990b)	267 ± 56	275 ± 26		
Benz *et al.* (1997)	235 ± 11			0.56 ± 0.04
This study			234–312	0.40–0.80

values. Using the Q^{-1} values computed from the tomographic model reduced the variance of the data by 11% to a level of 89% of the variance that occurred just using the average Q-value of 267.

The majority of η values fall between 0.4 and 0.8 (Table 1), suggesting a strong frequency-dependent attenuation in the Basin and Range Province. The low Q-values also indicate a region that is still tectonically active. The lowest Q_o values occur in the south and southwest part of the Basin and Range Province where active tectonic deformation is occurring today. Higher values occur in the east-central Basin and Range and the western margin of the Colorado Plateau. The areas with high Q_o values underwent volcanism between 17 and 55 m.y.a., while volcanism in low Q_o regions occurred less than 17 m.y.a. (Blackwell, 1978).

Acknowledgments

We thank William Walter for providing the set of Lawrence Livermore National Laboratory seismograms, and for a very thorough review. We also thank Robert B. Herrmann for providing us with programs to isolate the L_g spectra, Keith Koper for the genetic algorithm code used in this study, Patrick Shore for computer support, and Brian Shiro for his review of this work. This research was supported by the National Science Foundation, Grant Number EAR-9629018, and the David and Lucile Packard Foundation.

References

Al-Eqabi, G. I., K. Koper, and M. E. Wysession (2001). Source characterization of Nevada Test Site explosions and western U.S. earthquakes using L_g waves: implications for regional source discrimination, *Bull. Seism. Soc. Am.* **91,** 140–153.

Atkinson, G. M., and R. F. Mereu (1992). The shape of ground motion attenuation curves in southeastern Canada, *Bull. Seism. Soc. Am.* **82,** 2014–2031.

Baqer, S., and B. J. Mitchell (1998). Regional variation of L_g coda Q in the continental United States and its relation to crustal structure and evolution, *Pure Appl. Geophys.* **153,** 613–638.

Baumont, D., A. Paul, S. Beck, and G. Zandt (1999). Strong crustal heterogeneity in the Bolivian Altiplano as suggested by attenuation of L_g waves, *J. Geophys. Res.* **104,** 20287–20305.

Benz, H. M., A. Frankel, and D. M. Boore (1997). Regional L_g attenuation for the continental United States, *Bull. Seism. Soc. Am.* **87,** 606–619.

Blackwell, H. M. (1978) Heat flow and energy loss in the western United States, in *Cenozoic Tectonics and Geophysics of the Western Cordillera*, R. B. Smith and G. P. Eaton (Editors), *Geol. Soc. Am. Memoir*, Vol. 152, 175–208.

Chael, E. (1987). Spectral scaling of earthquakes in the Miramichi region of New Brunswick, *Bull. Seism. Soc. Am.* **77,** 347–365.

Chavez, D. E., and K. F. Priestley (1986). Measurement of frequency dependent L_g attenuation in the Great Basin, *Geophys. Res. Lett.* **13,** 551–554.

Cong, L., and B. J. Mitchell (1998). L_g coda Q and its relation to the geology and tectonics of the Middle East, *Pure Appl. Geophys.* **153,** 563–585.

Mitchell, B. J. (1991). Frequency dependence Q_{L_g} and its relation to crustal anelasticity in the Basin and Range Province, *Geophys. Res. Lett.* **18,** 621–624.

Mitchell, B. J. (1995). Anelastic structure and evolution of the continental crust and upper mantle from seismic surface wave attenuation, *Rev. Geophys.* **33,** 441–462.

Mitchell, B. J., and L. Cong (1998). L_g coda Q and its relation to the structure and evolution of the continents: a global perspective, *Pure Appl. Geophys.* **153,** 655–663.

Singh, S. K., and R. B. Herrmann (1983). Regionalization of crustal coda Q in the continental United States, *J. Geophys. Res.* **88,** 527–538.

Wyllie, P. J. (1988). Magma genesis, plate tectonics, and chemical differentiation of the Earth, *Rev. Geophys.* **26,** 370–404.

Xie, J., and B. J. Mitchell (1990a). A back-projection method for imaging large-scale lateral variations of L_g coda Q with application to continental Africa, *Geophys. J. Int.* **100,** 161–181.

Xie, J., and B. J. Mitchell (1990b). Attenuation of multiphase surface waves in the Basin and Range Province, part I, L_g and L_g coda, *Geophys. J. Int.* **102,** 121–137.

Department of Earth and Planetary Sciences
Washington University
St. Louis, Missouri 63130-4899

Manuscript received 6 May 2004.